



Three-Phase Induction Motor Speed Estimation Using Recurrent Neural Network Structure

Adam Islam Ridhatullah^{1*}, Ariffuddin Joret², Iradiratu Diah Prahmana Karyatanti¹, Asmarashid Ponniran²

¹Hang Tuah Surabaya University, Jl. Arief Rahman Hakim No.150, Surabaya, 60111, INDONESIA

²Universiti Tun Hussein Onn Malaysia, 86400 Parit Raja, Batu Pahat, Johor, MALAYSIA

*Corresponding Author

DOI: <https://doi.org/10.30880/jeva.2021.02.02.003>

Received 03 July 2021; Accepted 14 September 2021; Available online 30 December 2021

Abstract: In induction motor speed control method, the development of the field-oriented control (FOC) algorithm which can control torque and flux separately enables the motor to replace many roles of DC motors. Induction motor speed control can be done by using a close loop system which requires a speed sensor. Referring to the speed sensor weaknesses such as less accurate of the measurement, this is due to the placement of the sensor system that is too far from the control system. Therefore, a speed sensorless method was developed which has various advantages. In this study, the speed sensorless method using an artificial neural network with recurrent neural network (RNN) as speed observer on three-phase induction motor has been discussed. The RNN can maintain steady-state conditions against a well-defined set point speed, so that the observer is able and will be suitable if applied as input control for the motor drives. In this work, the RNN has successfully estimated the rotor flux of the induction motor in MATLAB R2019a simulation as about 0.0004Wb. As based on speed estimation error, the estimator used has produced at about 26.77%, 8.7% and 6.1% for 150rad/s, 200rad/s and 250rad/s respectively. The future work can be developed and improved by creating a prototype system of the induction motor to get more accurate results in real-time of the proposed RNN observer.

Keywords: Induction motor, speed sensorless, recurrent neural network

1. Introduction

The Induction motor is an alternate current (AC) motor that is often used in industry, such as in elevators, conveyors, blowers, pumps, et cetera [1]. Due to its reliability, low cost, and ease of maintenance, induction motor is commonly used worldwide. Especially after the development of field-oriented control (FOC) algorithm has made the induction motor replace the role of direct current (DC) motor in the industry [2]. Variable speed operation is required to operate the induction motor and closed-loop system is commonly used to obtain the variable speed. Therefore, a speed sensor system is required. But, the speed sensor system itself has disadvantages, such as inaccurate measurement due to the placement of the sensor system which is too far from the control system making it is ineffective for a control system with a big plant [3].

In last few years, FOC that had been applied in induction motor had gained high popularity worldwide, in its application of electric drive. For more than two decades, a significant effort has been put into AC drives field to remove the speed sensor which is on the motor shaft [4]. FOC control technique can be said to have a similarity to the DC motor control technique because it is possible to control flux and torque separately [2]. The sensorless control is considered as an important goal in the industry to obtain good performance at low cost [5], especially for operation on low performance and normal performance, sensorless control has been a standard in the industrial field. The advantages of speed sensorless

on the induction motor driver reduce the complexity of the device, low cost, and reduce the size of the machine drive, replace the cable sensor, does not make any noises, and reduce the cost of maintenance [6].

The artificial neural network (ANN) has shown a good result in becoming an alternative system modeling and parameter observer for induction motor. It can be seen that there are big differences based on ANN structure for each of the tasks [7]. The ANN is suitable for a non-linear control system where it can use approximation abilities for observing specific tasks [8]. The memory on the ANN is dependent on its weights and biases and can be classified into three categories base on how the weights and biases are obtained, such as fixed-weight, supervised, and unsupervised [9]. Regarding on this, this paper has discussed about speed sensorless induction motor control using ANN. The ANN types used is the recurrent neural network (RNN), which has been applied as a replacement for the speed observer of three-phase induction motor.

2. Three-Phase Induction Motor Modeling

The modeling of three-phase induction motor in this work is based on equation circuit which comprises of a - b - c coordinate system and d - q coordinate system.

2.1 a - b - c Coordinate System

The equivalent circuit of the three-phase induction motor is symmetrical if viewed by the rotating frame of the rotor circuit is as shown in Fig. 1. The stator circuit is described as the a_s , b_s , and c_s axes, while the rotor circuit is described as a_r , b_r , and c_r axes.

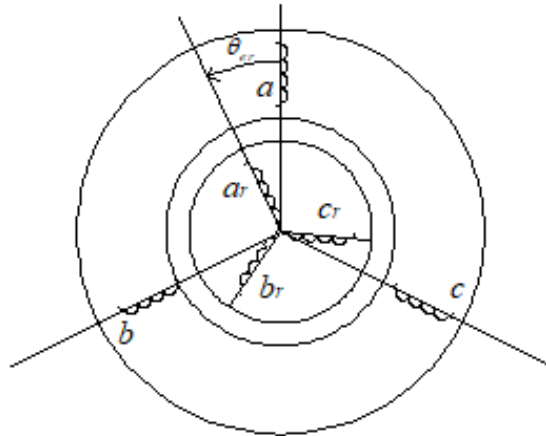


Fig. 1 - Stator and rotor of induction motor in a - b - c coordinate system

Stator and rotor voltage equation can be described as referring to Fig. 1 as:

$$V_{abcs} = r_s i_{abcs} + p \lambda_{abcs} \quad (1)$$

$$V_{abcr} = r_r i_{abcr} + p \lambda_{abcr} \quad (2)$$

where

$$p = \frac{d}{dt} \quad (3)$$

and

$$p \lambda_{abcs} = L_s i_{abcs} + L_s i_{abcr} \quad (4)$$

$$p \lambda_{abcr} = L_r i_{abcs} + L_r i_{abcr} \quad (5)$$

L_s and L_r matrix can be constructed as:

$$L_s = \begin{bmatrix} L_{ls} & -\frac{1}{2}L_{ms} & -\frac{1}{2}L_{ms} \\ -\frac{1}{2}L_{ms} & L_{ls} + L_{ms} & -\frac{1}{2}L_{ms} \\ -\frac{1}{2}L_{ms} & -\frac{1}{2}L_{ms} & L_{ls} + L_{ms} \end{bmatrix} \quad (6)$$

and

$$L_r = \begin{bmatrix} L_{lr} & -\frac{1}{2}L_{mr} & -\frac{1}{2}L_{mr} \\ -\frac{1}{2}L_{mr} & L_{ls} + L_{mr} & -\frac{1}{2}L_{mr} \\ -\frac{1}{2}L_{mr} & -\frac{1}{2}L_{mr} & L_{ls} + L_{mr} \end{bmatrix} \quad (7)$$

2.2 d-q Coordinate System

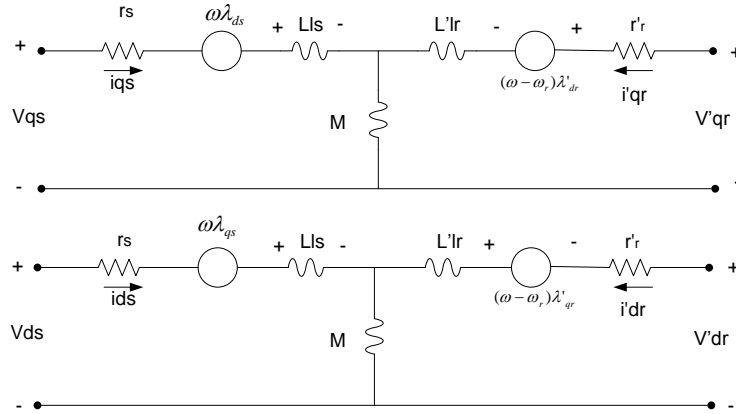


Fig. 2 - Equivalent circuit of d-q coordinate system of induction motor

Based on equivalence circuit in Fig. 2, the transformation of the *a-b-c* coordinate system to the *d-q* coordinate system of an three-phase induction motor can be calculated as given in equation 8 where *f* can be referred to as voltage, current or flux.

$$f_{qds} = T(\theta)f_{abcs} \quad (8)$$

The equation of stator voltage is

$$\bar{V}_s = R_s \bar{I}_s + \frac{d}{dt} \bar{\lambda}_s + j\omega_s \bar{\lambda}_s \quad (9)$$

where

$$\bar{V}_s = v_{ds} + jv_{qs} \quad (10)$$

$$\bar{I}_s = i_{ds} + ji_{qs} \quad (11)$$

$$\bar{\lambda}_s = \lambda_{ds} + j\lambda_{qs} \quad (12)$$

The equation of rotor voltage is

$$\bar{V}_r = R_r \bar{I}_r + \frac{d}{dt} \bar{\lambda}_r + j(\omega_s - \omega_r) \bar{\lambda}_r \quad (13)$$

where

$$\bar{V}_r = v_{dr} + jv_{qr} \quad (14)$$

$$\bar{I}_r = i_{dr} + ji_{qr} \quad (15)$$

$$\bar{\lambda}_r = \lambda_{dr} + j\lambda_{qr} \quad (16)$$

The equation of electromagnetic torque can be calculated as:

$$T_e = \frac{3pM}{2L_r} (\lambda_{rd} i_{sq} - \lambda_{rq} i_{sd}) \quad (17)$$

The motor angular speed is a function of electromagnetic torque and load torque is:

$$\frac{J}{p} \frac{d\omega_r}{dt} + K_g \omega_r = T_g - T_L \quad (18)$$

where,

K_g = the friction constant ($kg.m^2/dt$)

J = inertia moment ($kg.m^2$)

ω_r = rotor angular speed (rad/dt)

Linkage flux is described as a magnitude of rotating field on the coil within N winding.

$$\bar{\lambda}_s = L_s \bar{I}_s + M \bar{I}_r \quad (19)$$

$$\bar{\lambda}_r = L_r \bar{I}_r + M \bar{I}_s \quad (20)$$

The induction motor equation in the form of state variable equation can be simplified as:

$$\frac{d}{dt} \begin{bmatrix} i_s \\ \lambda_r \end{bmatrix} = \begin{bmatrix} A_{11} & A_{12} \\ A_{21} & A_{22} \end{bmatrix} \begin{bmatrix} i_s \\ \lambda_r \end{bmatrix} + \begin{bmatrix} B_1 \\ 0 \end{bmatrix} v_s = Ax + Bv_s \quad (21)$$

where

$$A_{11} = - \left\{ \frac{R_s}{\sigma L_s} + \frac{1-\sigma}{\sigma \tau_r} \right\} I = a_{r11} I \quad (22)$$

$$A_{12} = \frac{M}{\tau L_s L_r} \left\{ \frac{1}{\tau_r} I - \omega_r J \right\} = a_{r12} I + a_{i12} J \quad (23)$$

$$A_{21} = \left(\frac{M}{\tau_r} \right) I = a_{r21} I \quad (24)$$

$$A_{22} = - \left(\frac{1}{\tau_r} \right) I + \omega_r J = a_{r22} I + a_{i22} J \quad (25)$$

$$B_1 = \frac{1}{\tau L_s} I = b_1 I \quad (26)$$

$$C = [I \quad 0] \quad (27)$$

$$I = \begin{bmatrix} 1 & 0 \\ 0 & 1 \end{bmatrix} \quad (28)$$

$$J = \begin{bmatrix} 0 & -1 \\ 1 & 0 \end{bmatrix} \quad (29)$$

2.3 Induction Motor Simulation Model

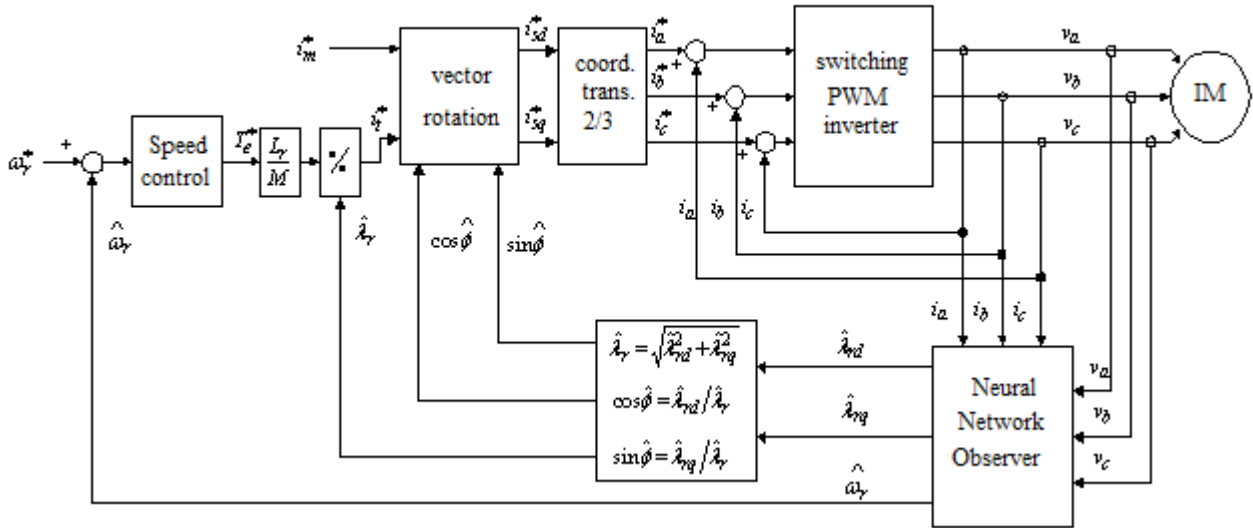


Fig. 3 - Block diagram system of induction motor simulation model

The block diagram of Fig. 3 was developed into a system modeling simulation in this work using the m-file from MATLAB R2019a. The three-phase motor specifications used for the simulation are:

- 115 Volt, 2 pairs of poles, 60 Hz.
- R_s = 176Ω; stator resistance
- R_r = 190Ω; rotor resistance
- L_s = 3.79H; stator inductance
- L_r = 3.31H; rotor inductance
- M = 3.21H; coupled inductance
- J = 1.05e-5kg.m²; inertia momen
- Kd = 1.49e-5kg.m²/s; friction constant

The equations used in the two-phase to three-phase coordinate transformation block are:

$$i_{ds}^* = i_{ds} \cos(\theta_e) - i_{qs} \sin(\theta_e) \tag{30}$$

$$i_{qs}^* = i_{ds} \sin(\theta_e) + i_{qs} \cos(\theta_e) \tag{31}$$

and

$$i_{as}^* = i_{qs}^* \tag{32}$$

$$i_{bs}^* = -\frac{\sqrt{3}}{2} i_{ds}^* - \frac{1}{2} i_{qs}^* \tag{33}$$

$$i_{cs}^* = \frac{\sqrt{3}}{2} i_{ds}^* - \frac{1}{2} i_{qs}^* \tag{34}$$

The PWM Inverter model has been made after making the induction motor model. The rotation vector concerning magnetizing current and torque current produces a reference phase current which is used for the inverter PWM control signal. The switching procedure applied in this work is as shown in Fig. 4, where the input of the pwm inverter has been set to 230V, -230V or 0V based on the error currents.

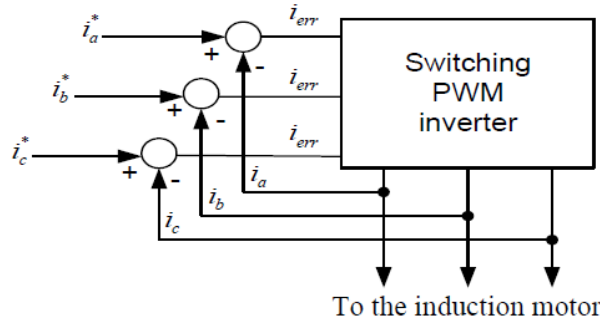


Fig. 4 - PWM inverter

2.4 Recurrent Neural Network

Recurrent neural network (RNN) is an ANN that can provide feedback to the neuron itself or other neurons. RNN has at least one feedback, where this feedback loop can affect the learning ability and performance of the network. In addition, the output of the RNN depends not only on the input at current time but also on the input of the previous time. This condition is intended so that the network can accommodate several events in the past, which are followed by a calculation process. This is important for more complex problems, the output of the neural network is time-varying so that the neural network has a time-sensitive response to past memory conditions.

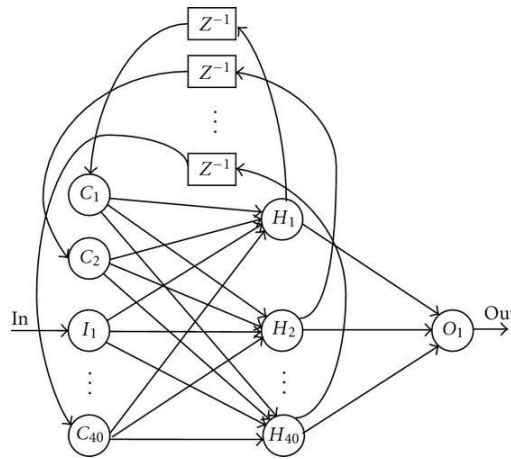


Fig. 5 - RNN structure

Based on RNN structure in Fig. 5, the output of the RNN can be calculated with the following equation:

$$y(k) = x(k + 1) - Ax(k) - V_1^0 \sigma[W_1^0 x(k)] - V_2^0 \phi[W_2^0 x(k)]u(k) \quad (35)$$

The flowchart of the RNN training used in this study is as shown in Fig. 6. The training is conducted in order to determine the suitable parameters of the RNN structure that best fit the rotor fluxes of the induction motor which has been simulated without the RNN estimator.

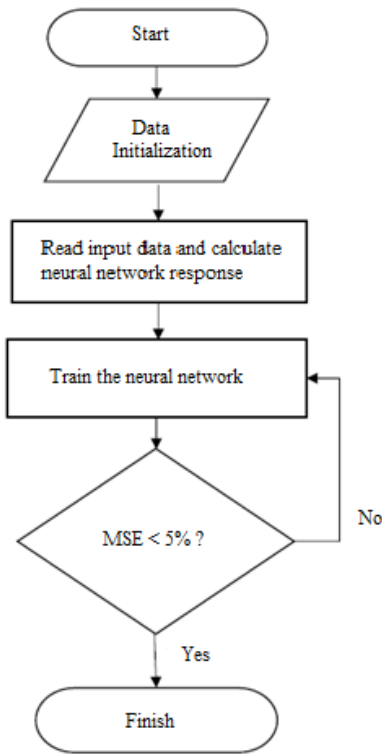


Fig. 6 - RNN training flowchart

2.5 Recurrent Neural Network Estimator

The flux estimation and identification of the speed of a three-phase induction motor in this work is based on neural network technique. The learning algorithm chosen is the back-propagation while the neural network structure used is the RNN. This network consists of three layers, namely the input layer, hidden layer, and output layer. The configuration during off-line training is to train the neural network observer using calculated rotor speed and direct and quadrature fluxes from an induction motor modeling. The configuration used can be seen in Fig. 7 and Fig. 8.

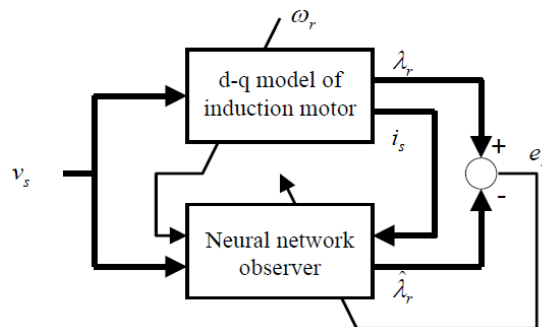


Fig. 7 - RNN observer offline training for flux estimation

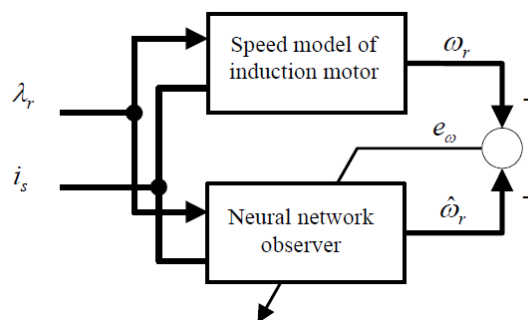


Fig. 8 - RNN observer offline training for speed identification

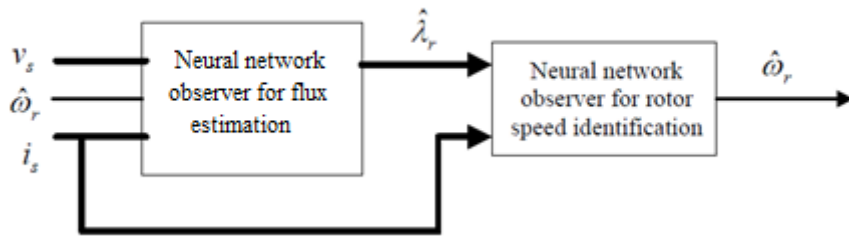


Fig. 9 - RNN observer for flux estimation and online rotor speed identification

The rotor speed identification when operating the simulation of the three-phase motor known as online, developed in this work can be seen in Fig. 9. In this work, the RNN observer has been used as a flux estimator so that the rotor flux which is a state variable of the induction motor model can be known and utilized in the control system. The observer of the RNN will use the variable equation of state of the induction motor to imitate the dynamics of the equation of the variable of the induction motor so that by studying the data obtained, the RNN can obtain the estimation values of flux and rotor speed.

3. Results and Discussion

In this study, the direct and quadrature fluxes of the rotor in the induction motor simulation without observer system (actual) and with RNN observer (blue) are as shown in Fig. 10–Fig. 15. Referring to these figures, the estimation of these rotor fluxes as made by the RNN seems to overlap with the actual signal. These results show that the use of the RNN estimator has perfectly estimated the flux of the rotor.

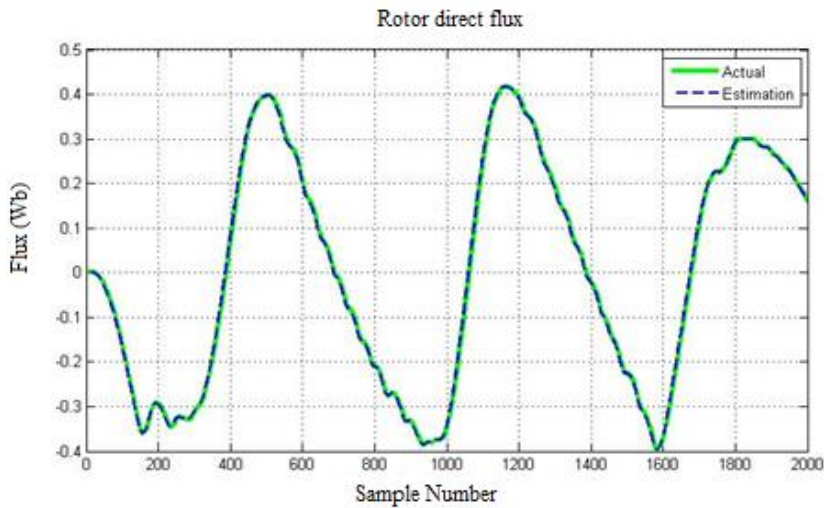


Fig. 10 - Rotor direct flux calculation at 150 rad/s

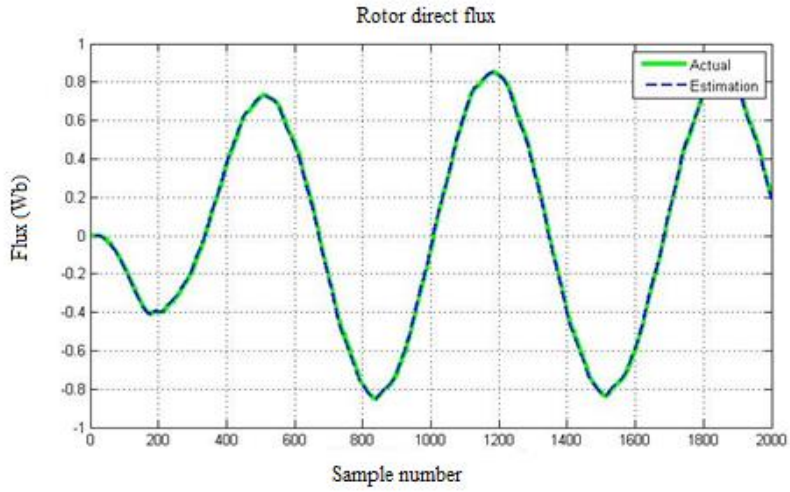


Fig. 11 - Rotor direct flux calculation at 200 rad/s

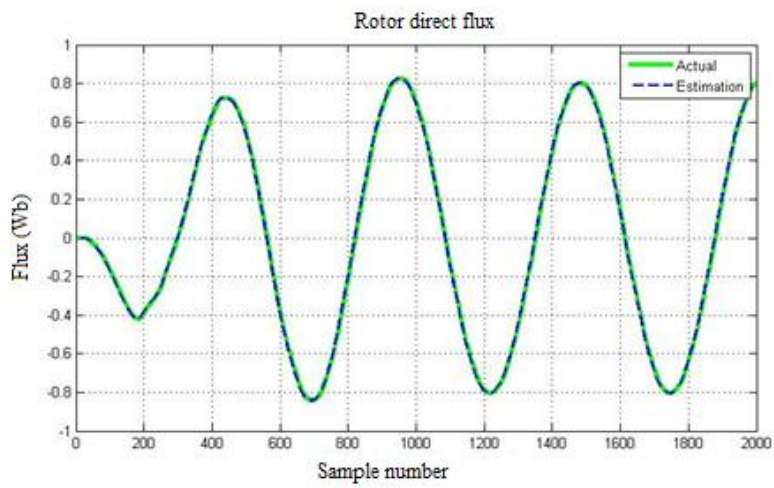


Fig. 12 - Rotor direct flux calculation at 250 rad/s

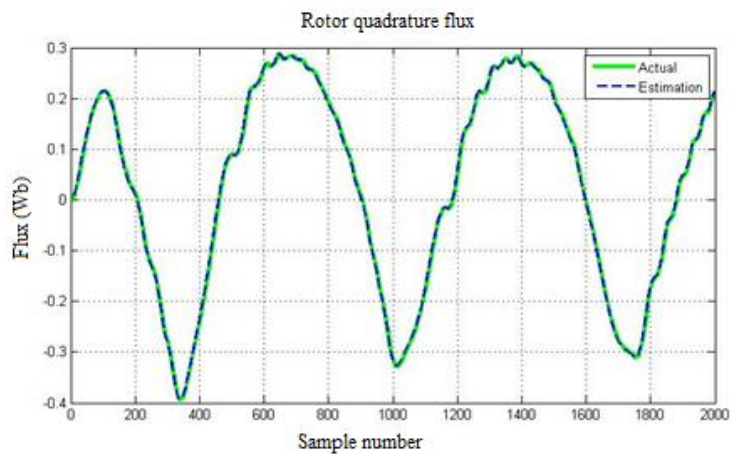


Fig. 13 - Rotor quadrature flux calculation at 150 rad/s

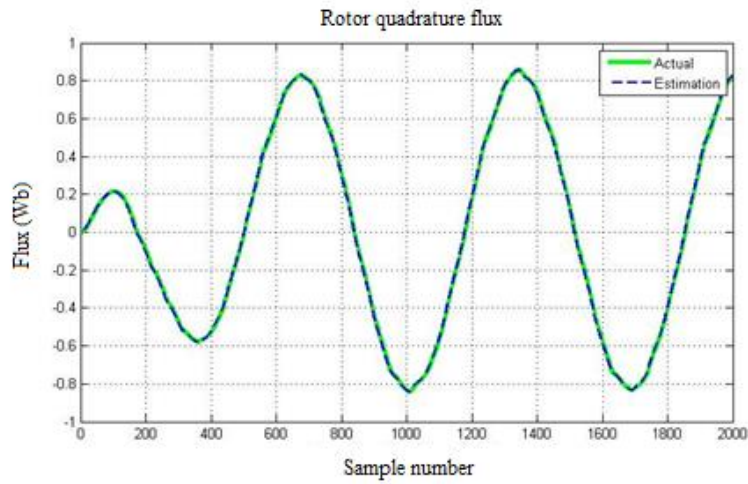


Fig. 14 - Rotor quadrature flux calculation at 200 rad/s

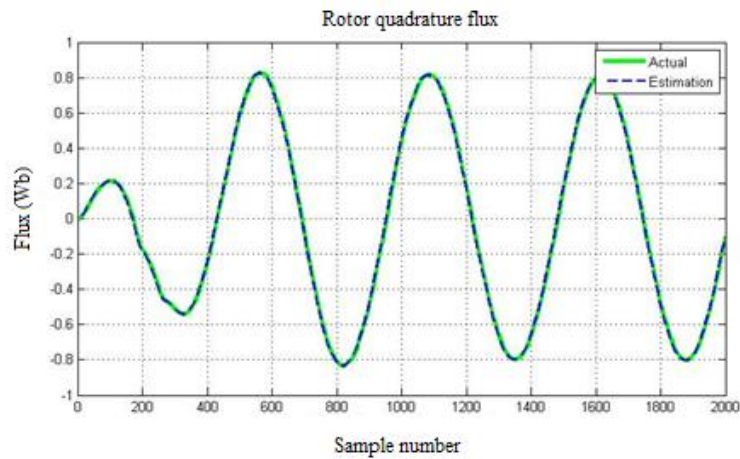


Fig. 15 - Rotor quadrature flux calculation at 250 rad/s

Based on the speed of the induction motor simulation with and without RNN estimator, the output speed from the RNN estimator has produced a constant speed profile with no ripple as compared to the speed calculation of the induction motor without controller system. This can be referred to Fig. 16-Fig. 18. Referring to the rotor speed calculation between the simulation with and without the RNN estimator in Fig. 16, the speed of the rotor at 150 rad/s without the estimator has produced transient at 450, 1100 and 1700 of sample number. As referring to the rotor direct flux calculation in Fig. 10, the transient can be observed to be happening as the polarity of flux changes from a negative value to a positive value which showing the changing state of the machine and to observe the transient condition when the machine operates out of the RNN working operation area. However, the transient did not occur when the machine runs at 200 rad/s and 250 rad/s. This is due to the initial parameters setting of the induction machine used in this study which can be said to be within the boundary of the RNN working operation area.

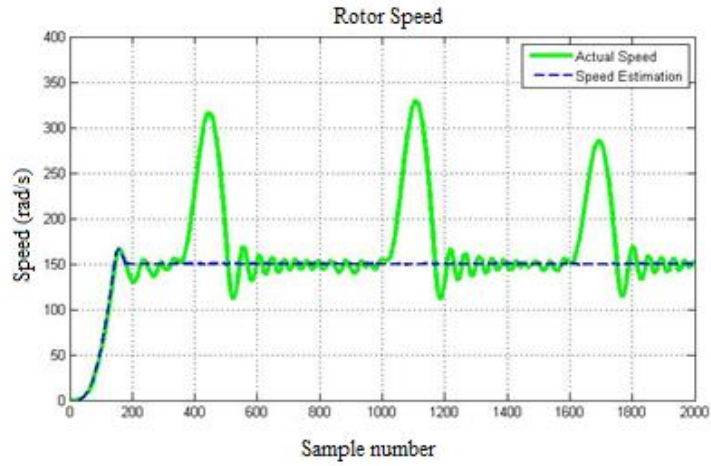


Fig. 16 - Rotor speed calculation at 150 rad/s

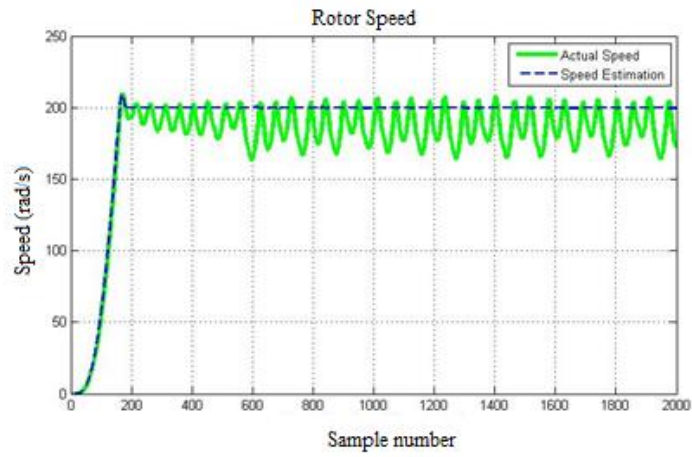


Fig. 17 - Rotor speed calculation at 200 rad/s

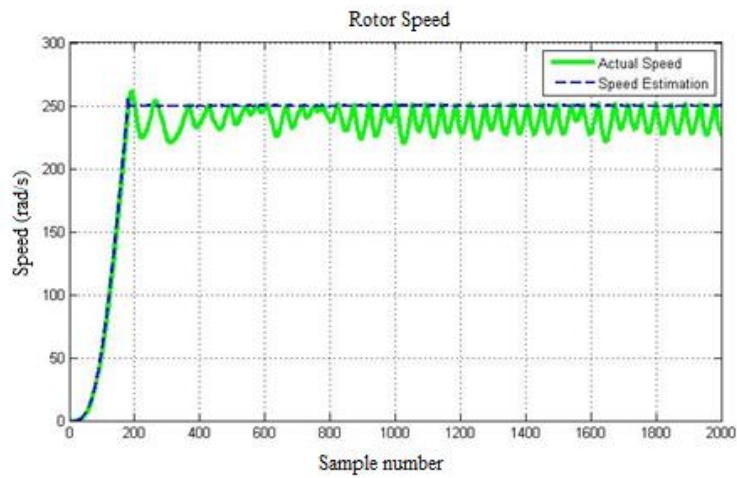


Fig. 18 - Rotor speed calculation at 250 rad/s

Table 4.1 - Recurrent neural network observer test online data at different speeds

No	ROTOR SPEED	MEAN SQUARE ERROR			
		FLUX DIRECT (Wb)	FLUX QUDRATURE (Wb)	SPEED (rad/s)	ERROR SPEED IN PERCENTAGE (%)
1	150 rad/s	0.0004309	0.0004308	40.1556	26.77
2	200 rad/s	0.00040	0.00043	17.412	8.7
3	250 rad/s	0.000375	0.000407	15.3456	6.1

Referring to Table 4.1, the mean square error (MSE) of the rotor rotational speed as estimated by the RNN observer is relatively small. Flux estimation in induction motor simulation using RNN observer with different speeds setting obtained the MSE value of the rotor direct flux ranging from 0.0004309 Wb to 0.0003745 Wb. Meanwhile, the MSE value for the rotor quadrature flux ranging from 0.0004308 Wb to 0.000407 Wb. Simulation of rotor speed identification using RNN observer applied in induction motor simulation with different speeds setting has obtained the MSE value ranging from 15.3456 rad/s to 40.1556 rad/s. The error percentages obtained through the RNN method of controlling are 6.1% at speed of 250 rad/s, 8.7% at speed of 200 rad/s, and 26.77% at speed of 150 rad/s.

4. Conclusion

Simulation of an induction motor controller using RNN estimator using MATLAB software has been successfully developed. Based on the results of the simulation the fluxes of the rotor has been perfectly estimated by the estimator with error value at about 0.0004 Wb. Referring to the speed profile of the induction motor simulation in this study, it is known that the result of MSE speed is relatively large because it exceeds 5%. As for improvement, the RNN estimator can be retrained or modified in term of its training algorithm and structure. However, the RNN can maintain steady-state conditions against a well-defined set point speed, so that the observer is able and will be suitable if applied as input control for an induction motor drives.

Acknowledgement

The authors would like to extend their gratitude to Universiti Tun Hussein Onn Malaysia (UTHM) and Hang Tuah Surabaya University for supporting this research study under Student Mobility Programme.

References

- [1] M. Aswin, Perancangan Pengendali Field-Oriented Controller (FOC) Motor Induksi Tanpa Sensor Berbasis Model Reference Adaptive System (MRAS), Malang: Universitas Muhammadiyah Malang, 2019
- [2] L. Fan and Y. Liu, "Neural Network-Based Speed Identification For Speed-Sensorless Induction Motor Drives," in *Chinese Control and Decision Conference*, Xuzhou, 2010
- [3] I.D.P. Karyanti, Perancangan Neural Network Observer Untuk Identifikasi Kecepatan Motor Induksi, Surabaya: Institut Teknologi Surabaya, 2003
- [4] Y. B. Zbede, S. M. Gadoue and D. J. Atkinson, "Model Predictive MRAS Estimator for Sensorless Induction Motor Drives," *IEEE Transactions On Industrial Electronics*, pp. Vol. 63, No. 6, pp. 3511-3521, 2016
- [5] S. Bodkhe and M. Aware, "Speed-Sensorless, Adjustable-Speed Induction Motor Drive Based on DC-Link Measurement," *International Journal of Physical Sciences*, pp. Vol. 4, No. 4, pp. 221-232, 2009
- [6] H. Kreiem, M. B. Hamed, L. Sbita and M. N. Abdelkrim, "DTC Sensorless Induction Motor Drives based on MRAS Simultaneous Estimation of Rotor Speed and Stator Resistance," *International Journal of Electronica and Power Engineering*, pp. Vol. 2, No. 5, pp. 306-313, 2008
- [7] J. M. Gutierrez-Villalobos, J. Rodriguez-Resendiz, E. A. Rivas-Araiza and V. H. Muciho, "A Review of Parameter Estimators and Controllers For Induction Motors Based On Artificial Neural Networks," pp. Vol.118, pp. 87-100, 2013
- [8] O. Elbeji and M. B. Hamed, "Sensorless Vector Control of Permanent Magnet Synchronous Motor Using Neural Network Observer," in *2017 International Conference on Green Energy Conversion Systems (GECS)*, Hammamet, 2017

- [9] Y. Oguz and M. Dede, "Speed Estimation of Vector Controlled Squirrel Cage Asynchronous Motor," *Energy Conversion and Management*, pp. Vol. 52, No. 1, pp. 675-686, 2011
- [10] H. Al-Bahadili, M. E. Dubakh, and A. M. Abbass, "Three-phase Induction Motor Speed Estimator Using Genetic Algorithm Based on Elman Recurrent Neural Network," in *2019 3rd International Symposium on Multidisciplinary Studies and Innovative Technologies (ISMSIT)*, Ankara, 2019
- [11] Y. Yang, "A neural network model reference adaptive system for speed estimation of sensorless induction motor," *2017 29th Chinese Control And Decision Conference (CCDC)*, 2017, pp. 6864-6868, doi: 10.1109/CCDC.2017.7978416
- [12] M. H. Zulkarnain, Peramalan Beban Listrik Jangka Panjang Pada PT. PLN (Persero) APJ Jember Dengan Menggunakan Metode Recurrent Neural Network Dengan Optimasi Levenberg Marquardt, Jember: Universitas Jember, 2018
- [13] S. Z. Zhekov, "Sensorless Indirect Neural Control of Induction Motor," in *2018 IEEE XXVII International Scientific Conference Electronics - ET2018*, Sozopol, Bulgaria, 2018
- [14] D. R. Baskoro, Peramalan Jangka Pendek Beban Tenaga Listrik Pada PT. PJB Gresik Menggunakan Metode Constructive Backpropagation Neural Network Serta Prediksi Kebutuhan Bahan Bakar Gas Pembangkitan, Jember: Universitas Jember, 2017
- [15] S. Wang, W. Huang, Y. Zhao, "An Extended-State-Observer-Compensated Extended-Kalman-Filter Sensorless Control for Asynchronous Generator", *Electrical Machines and Systems (ICEMS) 2020 23rd International Conference on*, pp. 1178-1183, 2020